Fig. S1

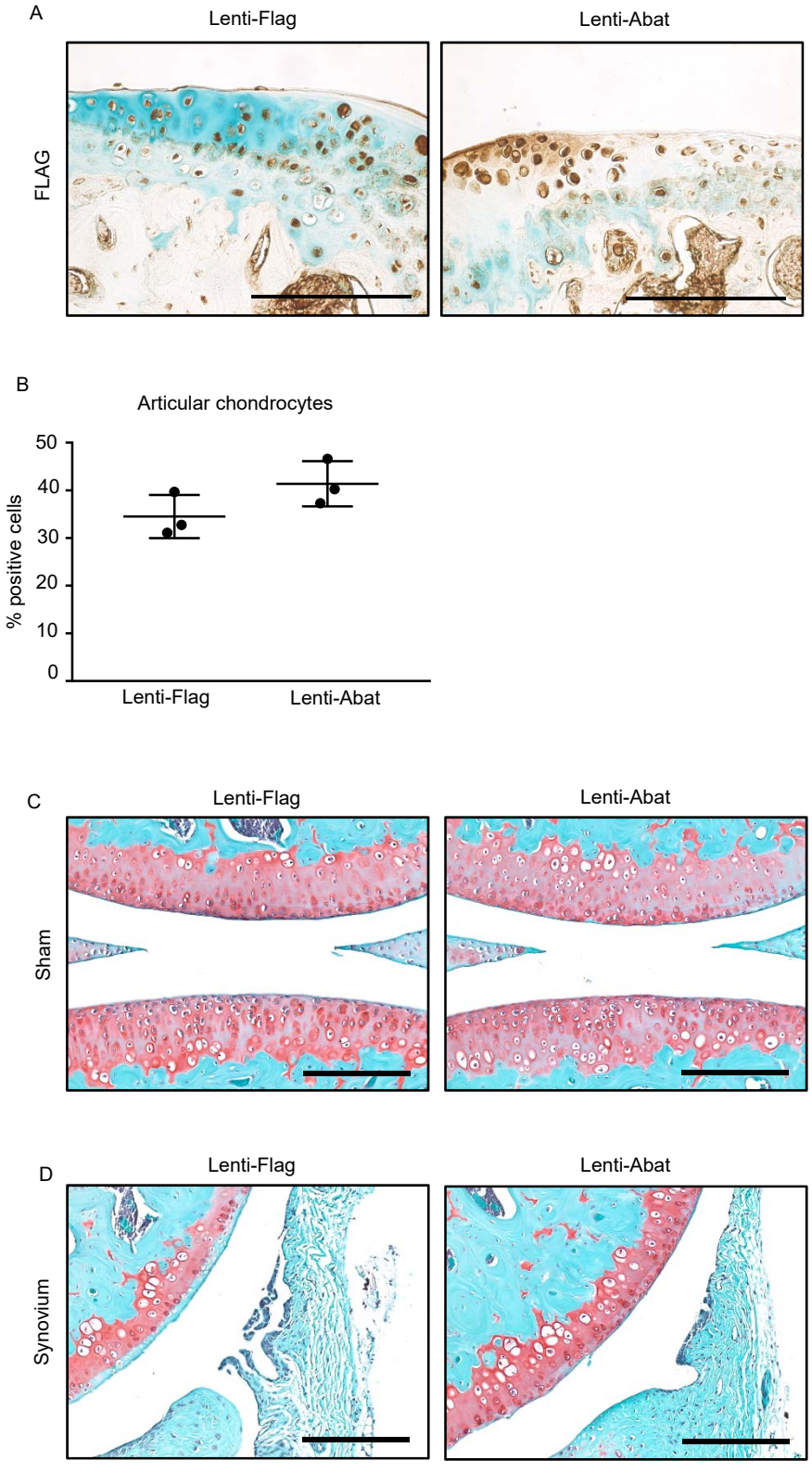
A
Lenti-Flag
Lenti-Abat
FLAG
B
Articular chondrocytes
% positive cells
50
40
30
20
10
0
Lenti-Flag
Lenti-Abat
C
Lenti-Flag
Lenti-Abat
Sham
D
Lenti-Flag
Lenti-Abat
Synovium

Fig. S1. Abat/FLAG is expressed in joint tissues. (A) Immunohistochemical analysis for Abat/FLAG expression on knee sections of control and Abat GOF cartilage. (B) Quantification of FLAG positive articular chondrocytes in MLI knee joints (n=3). (C) Representative images of histological sections of control and Abat GOF knee joints from sham surgeries (n=7). (D) Representative images of synovium tissue from control and Abat GOF knee joints at 4 weeks following MLI surgery (n=7). Scale bar, 50 μm.

Fig. S2

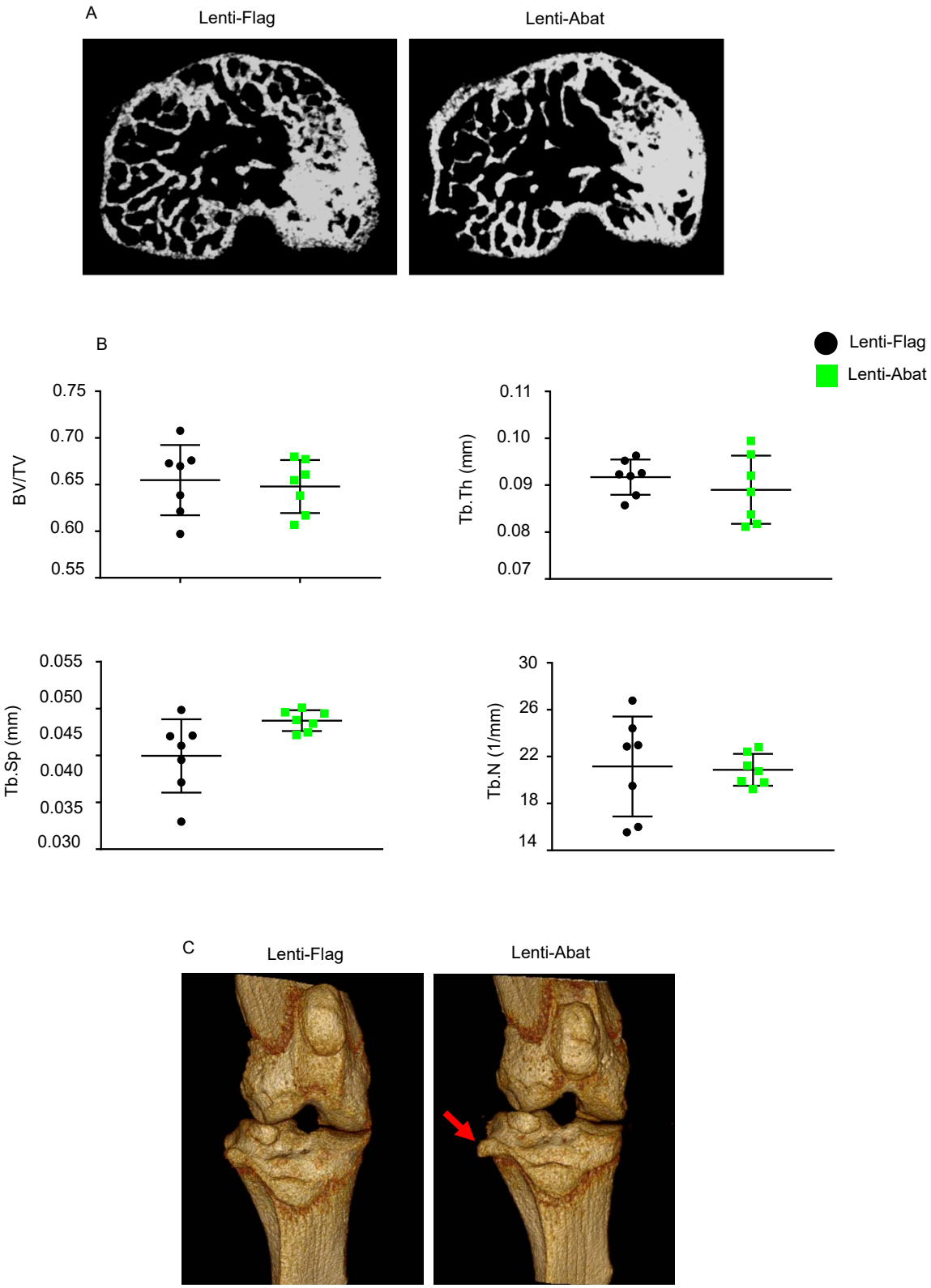
A
Lenti-Flag
Lenti-Abat
B
Lenti-Flag
Lenti-Abat
BV/TV
0.75
0.70
0.65
0.60
0.55
Tb.Th (mm)
0.11
0.10
0.09
0.08
0.07
Tb.Sp (mm)
0.055
0.050
0.045
0.040
0.035
0.030
Tb.N (1/mm)
30
26
22
18
14
C
Lenti-Flag
Lenti-Abat

Fig. S2. Micro-CT analyses reveal osteophyte formation in Abat GOF mice. (A) Representative images of subchondral bone from control and Abat GOF knee at 4 weeks post MLI. (B) Quantification of subchondral bone from medial tibial plateau, including BV/TV, Tb.Th, Tb. Sp and Tb. N (n=7). (C) Representative image of knee joints from control and Abat GOF knee at 4 weeks post MLI. Red arrow denotes osteophyte formation. Red arrow, osteophyte.

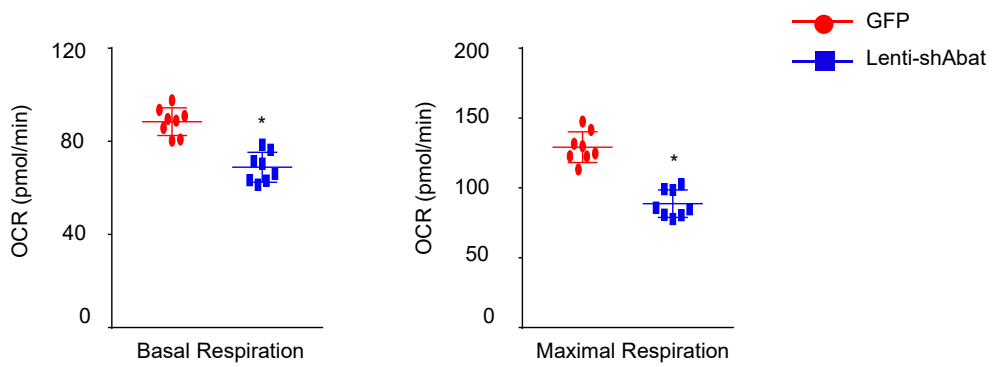

Fig. S3. Mitochondrial respiration is suppressed by Abat inhibition. The mitochondria respiration was measured in primary articular chondrocytes treated with lenti-GFP (Ctrl) and lenti-shAbat (Abat inhibition). Basal respiration and maximal respiration, as measured by the oxygen consumption rate (OCR) are shown ($n = 8$). *$p < 0.05$ by two-tailed Student's t test.

Fig. S4

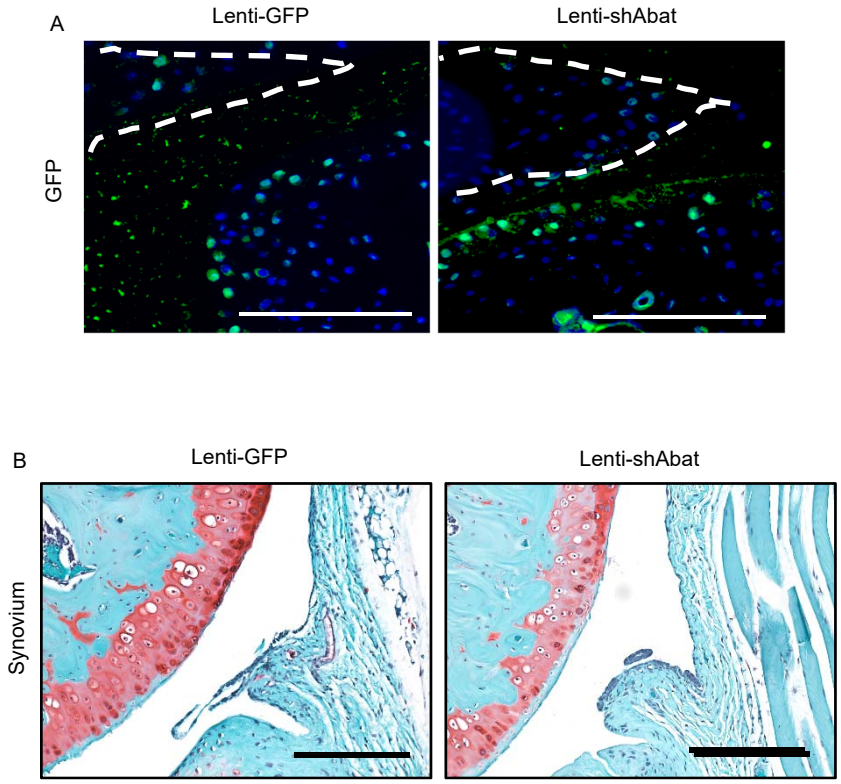

Fig. S4. shAbat/GFP is expressed in joint tissue. (A) Immunohistochemical analysis of GFP expression in knee sections of control and Abat LOF cartilage. White line denotes meniscus tissue. (B) Representative images of synovium tissue from control and Abat LOF knee joints at 10 weeks following MLI surgery (n=7). Scale bar, 50 μm.

Fig. S5

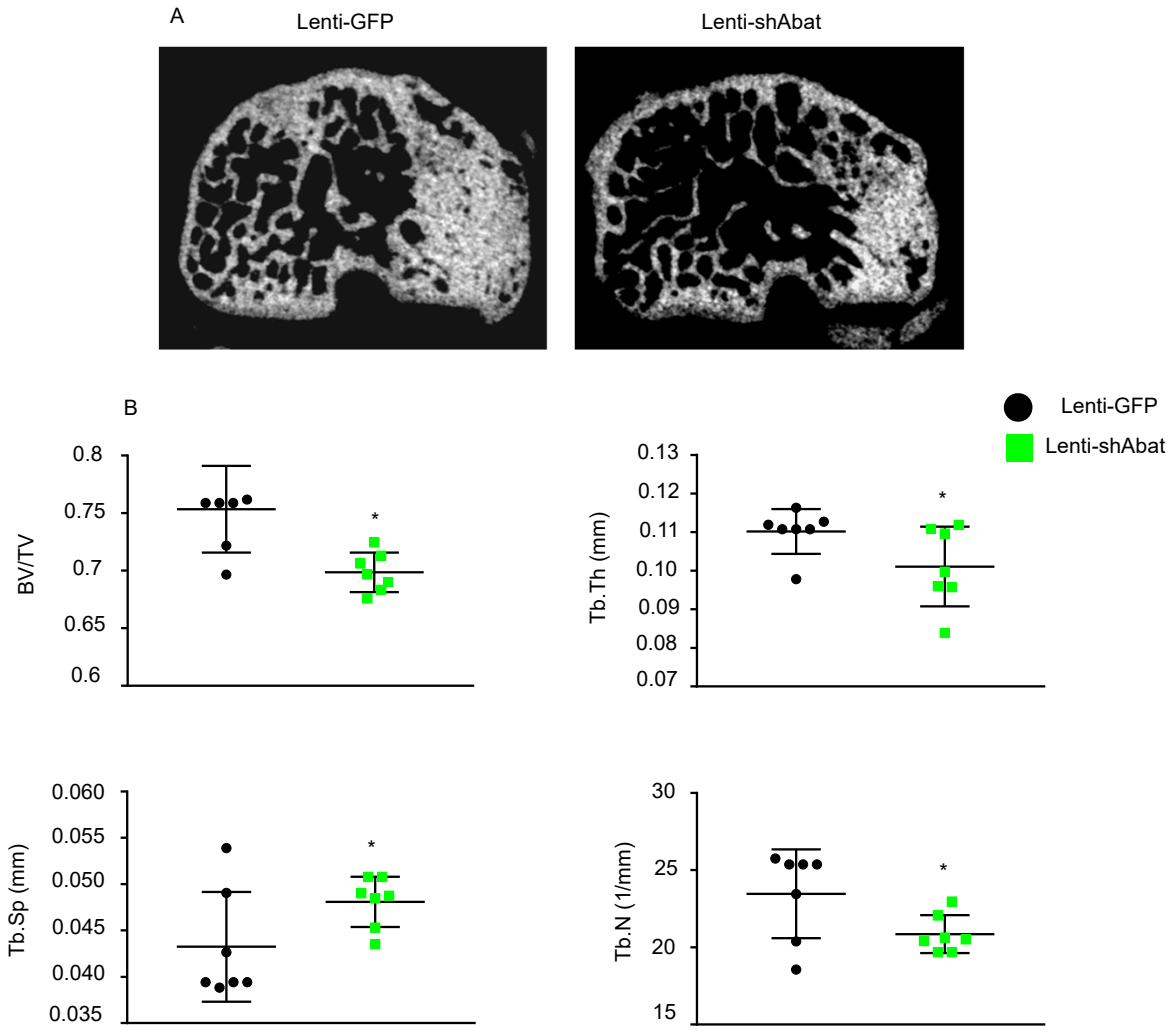

Fig. S5. Micro-CT analysis reveals reduced subchondral sclerosis in Abat LOF mice. (A) Representative images of subchondral bone from control and Abat LOF knee at 10 weeks post MLI. (B) Quantification of subchondral bone from medial tibial plateau, including BV/TV, Tb.Th, Tb. Sp and Tb. N (n=7). *$p < 0.05$ by two-tailed Student's *t* test.

Fig. S6

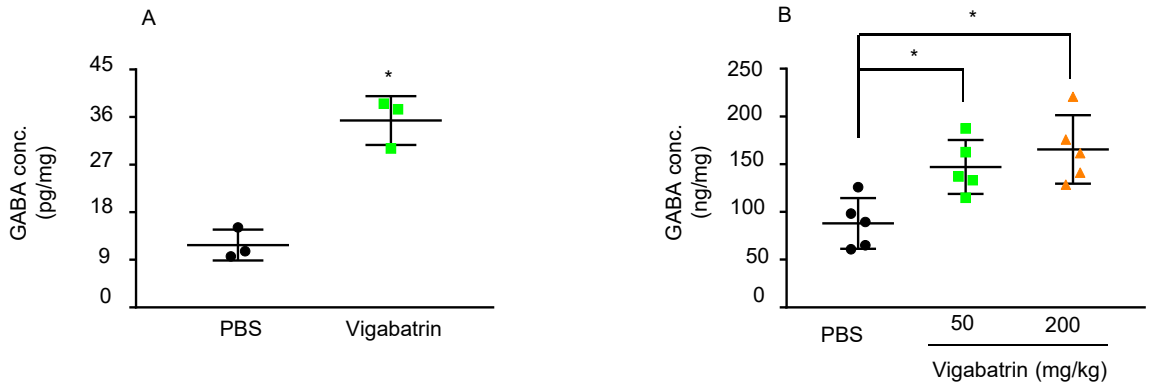

Fig. S6. Vigabatrin increases GABA concentration *in vivo* and *in vitro*. (A) GABA concentration is increased in brain tissues from Vigabatrin treated mice (n=5). (B) Cellular GABA concentration is increased in primary chondrocytes treated with vigabatrin (100uM) for 24 hours (n=3). *$p < 0.05$ by two-tailed Student's *t* test.

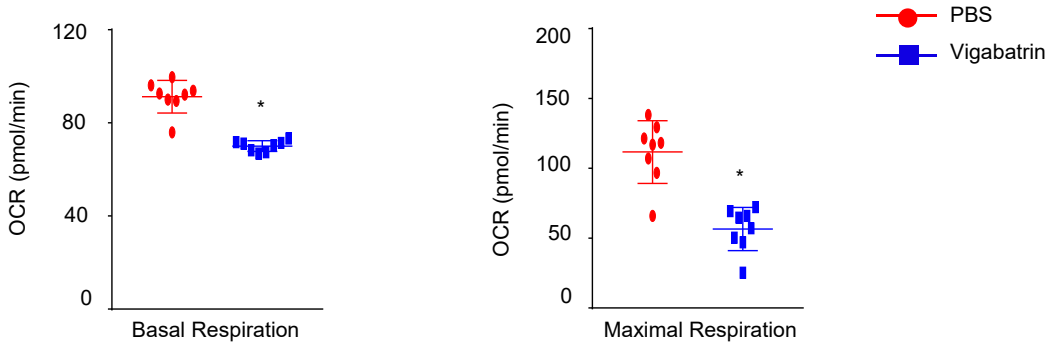

Fig. S7. Vigabatrin reduces chondrocyte mitochondria respiration. The mitochondria respiration was measured in primary articular chondrocytes treated with PBS and Vigabatrin. Basal respiration and maximal respiration, as measured by the oxygen consumption rate (OCR) are shown ($n = 8$). *$p < 0.05$ by two-tailed Student's *t* test.

Fig. S8

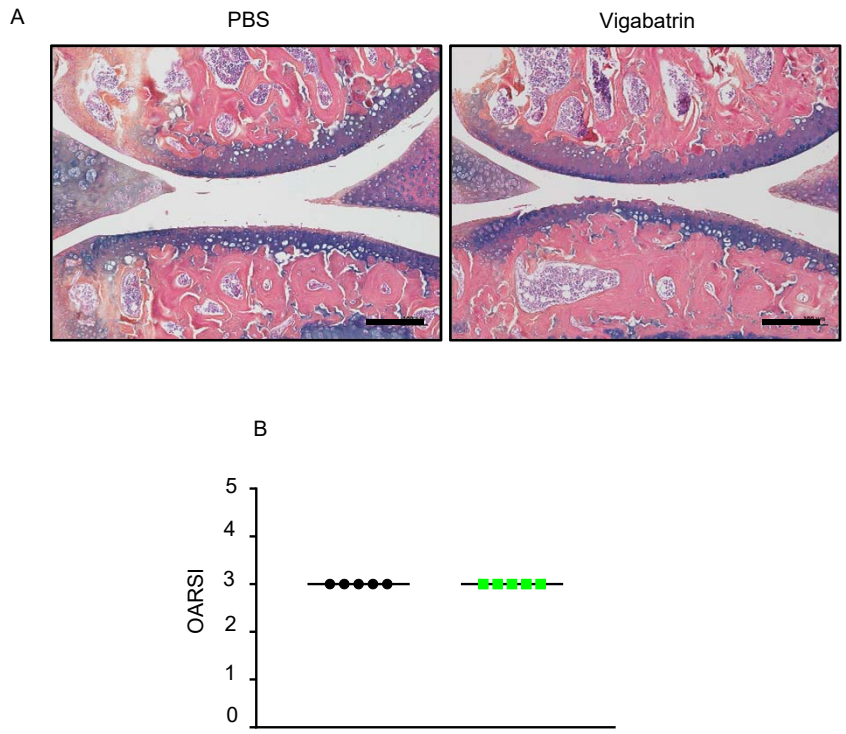

Fig. S8. Low dose of Vigabatrin does not protect cartilage degeneration. (A) Representative images of histological sections of PBS and Vigabatrin (50mg/kg) treated knee joints at 6 weeks following MLI surgery (n=5). (B) Quantification of histological assessment by OARSI scoring (n=5). Scale bar, 50 μm.

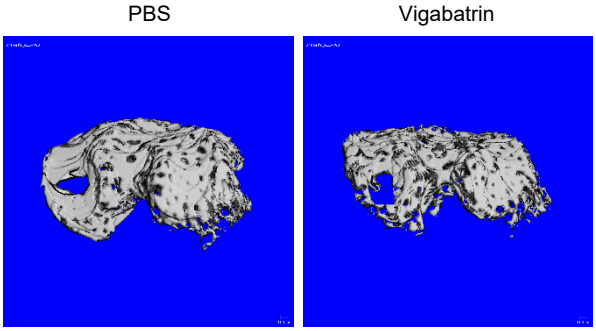

Fig. S9. Vigabatrin reduces subchondral bone sclerosis induced by MLI surgery. Representative micro-CT images for subchondral bone in PBS and Vigabatrin treated mice at 10 weeks following MLI surgery (n=5).

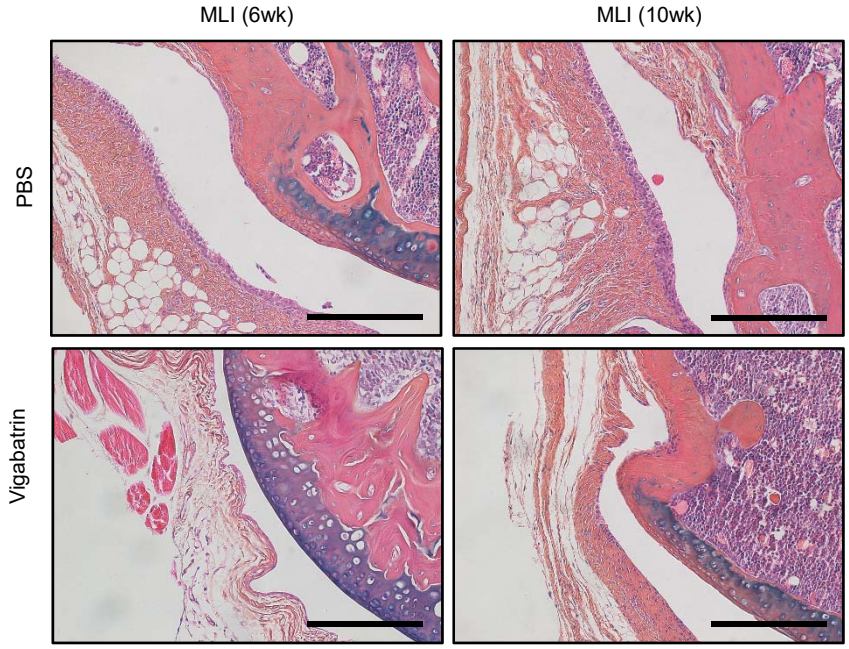

Fig. S10. Vigabatrin reduces synovial inflammation induced by MLI surgery.

Representative images of synovium tissue from PBS and Vigabatrin treated mice following MLI surgery (n=5). Scale bar, 50 μm.

Data file S1. Forty-four genes with differentially expressed methylation and mRNA